Available online at www.sciencedirect.com
ScienceDirect
Journal of Hazardous Materials 147 (2007) 1028–1036
Journal of Hazardous Materials
www.elsevier.com/locate/jhazmat

Studies on the adsorption of reactive brilliant red X-3B dye on organic and carbon aerogels

Xinbo Wu [a], Dingcai Wu [a], Ruowen Fu [a,b,*]

[a] *Materials Science Institute, PCFM Laboratory, School of Chemistry and Chemical Engineering, Sun Yat-sen University, Guangzhou 510275, PR China*
[b] *Institute of Optoelectronic and Functional Composite Materials, PR China*

Received 22 November 2006; received in revised form 25 January 2007; accepted 26 January 2007
Available online 6 February 2007

Abstract

Organic aerogels (AGs) and carbon aerogels (CAs) as adsorbents were successfully fabricated by a sol–gel polymerization method. The BET specific surface area and pore size distribution of the samples were analyzed by N_2 adsorption measurements. The adsorption efficiency of prepared samples towards reactive brilliant red X-3B dye (RBRX) was investigated. The adsorption of dye was found to follow the Langmuir and Freundlich models. The thermodynamic parameters, such as the change of free energy, enthalpy and entropy were calculated from equilibrium constants. Kinetic studies indicated that the adsorption of CA followed pseudo first and second order kinetic model, but the adsorption of AG only followed pseudo first order kinetic model. Batch adsorption studies were conducted to evaluate the effects of main preparation and adsorption conditions such as R/C (molar ratio of resorcinol (R) to surfactant (CTAB)) of adsorbent, pH, adsorbent dose and adsorbent particle size on the adsorption of RBRX on AG and CA. The results showed that the adsorption capacity of dye increased with the decrease in dose and particle size of the adsorbent. Maximum adsorption of AGs and CAs was observed at R/C = 200. The adsorption capacity of AG and CA would increase largely when pH < 4 or pH > 12.

Keywords: Adsorption; Reactive dye; Organic and carbon aerogels

1. Introduction

The effluents of wastewater in some industries such as dyestuff, textiles, leather, paper, plastics, etc., contain various kinds of synthetic dyestuffs. Among textile effluents, reactive dyes are hardly eliminated under aerobic conditions and are probably decomposed into carcinogenic aromatic amines under anaerobic conditions [1]. Furthermore, it is difficult to remove reactive dyes using chemical coagulation due to the dyes' high solubility in water [2]. A very small amount of dye in water is highly visible and can be toxic to creatures in water [3]. Hence, the removal of color from process or waste effluents becomes environmentally important. Among some existing technologies, adsorption has been shown to be an effective technique with its high efficiency, capacity and applicability on a large scale to remove dyes as well as having the potential for regeneration, recovery and recycling of adsorbents. Many studies have been undertaken to find suitable adsorbents to lower dye concentrations from aqueous solutions [4–9]. Removal of dyes from aqueous solutions using activated carbons by adsorption process is currently of great interest [10–12].

Recently, a new form of carbon adsorbent—carbon aerogel (CA) has appeared [13,14]. CAs are novel mesoporous carbon materials with many interesting properties, such as low mass densities, continuous porosities, high surface areas, great mesopore volume and high electrical conductivity [15,16]. These properties are derived from their three-dimensional nano-network structures. CAs and their organic aerogel (AGs) precursors are new and emerging adsorbent materials composed of covalently bonded nanometer sized particles that are arranged in three-dimensional network and have high porosity and high surface area. They may be produced in solid shapes, powder and sheet forms and provide excellent treatment efficiency in a cost effective manner for the purification of wastewaters. CAs and AGs have been reported for the adsorption of inorganic

* Corresponding author at: Materials Science Institute, Sun Yat-sen University, Guangzhou 510275, PR China. Tel.: +86 20 84115112; fax: +86 20 84115112.
E-mail address: cesfrw@zsu.edu.cn (R. Fu).

0304-3894/$ – see front matter © 2007 Elsevier B.V. All rights reserved.
doi:10.1016/j.jhazmat.2007.01.139

(especially metal ions) [17–20], theophylline [13] and organic vapors [14], but its use for the removal of organic dyes has few reported. It is therefore desirable to explore the application of treatment of organic dye use AGs and CAs as a kind of new adsorption materials.

In previous studies, our research groups have successfully obtained good results about improving technics and reducing cost in the process of preparation of AGs and CAs [21,22]. The main objective of this study was to investigate the feasibility of using AG and CA materials for the adsorption of a model adsorbate RBRX from aqueous solution. The adsorption equilibrium data were obtained to discover which isotherm model provided the best fitting for this adsorption process. In order to predict and design the adsorption process more exactly, we have studied the adsorption kinetics and thermodynamics under various experimental conditions. The effects of main preparation and adsorption conditions, such as R/C (molar ratio of resorcinol (R) to surfactant (CTAB)) of adsorbent (the key factor that influences the pore structure and distribution of AG and CA), pH of the RBRX solution, adsorbent dose, adsorbent particle size, on the adsorption of RBRX are studied in order to determine the optimum process conditions. The information obtained would be expected to be useful for environmental technologists in designing reactive dye containing wastewater treatment systems.

2. Experimental

2.1. Adsorbate

The textile dye, RBRX was from Shanghai Eighth Dyestuffs Co., Ltd. of China, and it was used as received without further purification. Stock solutions were prepared by dissolving accurately weighed 8.000 g (±0.0015 g) of dye in 1 dm^3 of distilled water. The experimental solutions of desired concentration were obtained by successive dilutions with double-distilled water. The molecular structure of RBRX is shown in Fig. 1.

2.2. Preparation of adsorbents (AGs and CAs)

The preparation of AGs as follows: 165 g resorcinol (R), 207.9 mL formaldehyde (F) and appropriate surfactant (CTAB) were mixed with 240.9 mL water according to predetermined recipes, and then transferred into a 600 mL glass vial. The vial was sealed and then put into a water bath at 70 °C to cure for one day and then cure for 5 days at 85 °C. After curing, the sample were directly dried in the air at room temperature for 2 days at first, and further dried under an infrared lamp with an irradiation temperature at about 60 °C for 24 h, and finally dried in an oven at 105 °C under ambient pressure for 3 h.

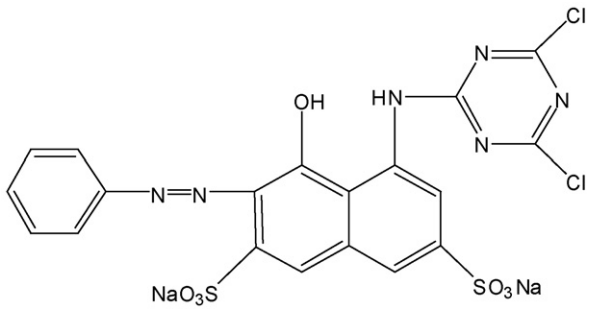

Fig. 1. Structure of RBRX (chemical formula: $C_{19}H_{10}O_7N_6Cl_2S_2Na_2$; molecular weight: 615).

CAs were prepared by related AGs which was heated to 900 °C with a heating rate of 5 °C/min and kept at this carbonization temperature for 3 h in flowing N_2 (800 mL/min).

All samples were broken to 20–40 mesh except special request.

2.3. Measurement of the pore parameters and pore size distribution

Approximately 0.12 g samples were heated to 150 °C for the AG, or to 250 °C for the CA to remove all the adsorbed species. Nitrogen adsorption and desorption isotherms were then taken using an ASAP 2010 Surface Area Analyzer (Micromeritics Instrument Corporation). According to the resulting isotherms, the BET surface area (S_{BET}), micropore volume (V_{mic}), micropore surface area (S_{mic}), mesopore volume (V_{BJH}), mesopore surface area (S_{BJH}), and pore size distribution of the samples were analyzed by Brunauer–Emmett–Teller (BET) theory, *t*-plot theory, Barrett–Johner–Halendar (BJH) theory, and density functional theory (DFT) theory, respectively.

2.4. Adsorption experimental methods and measurements

In experiments of equilibrium adsorption isotherm, 0.1 g adsorbent and 50 mL dye solution of desired concentration were put in a flask (100 mL), and were shaken for 24 h using an incubator shaker operating at 153 rpm at different temperatures. In experiments of kinetic adsorption, 0.3 g adsorbent and 150 mL dye solution of 800 mg/L initial concentration were put in a flask (250 mL) at a constant temperature of 30 °C. The 1 mL sample was carefully withdrawn from the flask at predetermined time intervals using a digital micropipette. In conditional experiments, 0.1 g adsorbent and 50 mL dye solution of 800 mg/L initial concentration were put in a 100 mL flask, and shaken for 24 h using shaker operating at 153 rpm at a constant temperature of 30 °C.

The effect of pH was studied by adjusting the pH of dye solutions using dilute HC1 and NaOH solutions. For AG and CA samples in all experiments except for that on the effect of R/C, the R/C is 125.

All RBRX solutions were diluted with distilled water and analyzed by a UV/VIS spectrophotometer (756, China) at a maximum wavelength of 538 nm. The final concentration of the solution was then determined from the calibration curve. The dye adsorption capacity at equilibrium, q_e (mg/g), can be calculated from

$$q_e = \frac{V(C_0 - C_e)}{m} \quad (1)$$

where C_0 (mg/L) is the initial dye concentration in liquid phase, C_e (mg/L) is the dye concentration in liquid phase at equilibrium, V (L) is the total volume of dye solution and m (g) is the mass of adsorbent.

3. Results and discussion

3.1. Characteristic of prepared adsorbents

According to N_2 adsorption and desorption isotherms, the specific surface area, specific pore volume and pore size distribution of the samples were obtained and the results were shown in Table 1 and Fig. 2. It is evident that AG and CA that we prepared are typical mesopore materials. From Fig. 2, we can see that the AG and CA samples obtained have a different pore size distribution in the range of micropore and a very similar pore size distribution in the range of mesopore. This indicates that the micropores in the CA are mainly produced during carbonization. The carbonization process changes the aerogel structure from thermosetting polymer to amorphous carbon. During carbonization, a large number of small molecule compounds such as carbon monoxide, carbon dioxide, and water are released due to the burnout of the organic groups, which leads to the creation of new micropores or voids in the gel. We can also find from Table 1 that the BET specific surface area of the CA is great larger than that of its precursory AG. The reason is that the carbonization step reduces the number of macropores (due to shrinkage) and increases the number of micropores (most likely due to the release of small molecule compounds) and mesopores (resulting from the shrinkage of some macropores), which leads to an increase in the surface area of CAs.

Table 1
Textual characteristics of the representative samples in the study

Sample	AG-125	CA-125
S_{BET} ($m^2\ g^{-1}$)	296.1	582.7
S_{micro} ($m^2\ g^{-1}$)	37.8	312.8
S_{BJH} ($m^2\ g^{-1}$)	291.3	302.1
V_{micro} ($cm^3\ g^{-1}$)	0.0136	0.145
V_{BJH} ($cm^3\ g^{-1}$)	1.216	1.150
dp (4V/A by BJH) (Å)	167.0	152.3
dp (4V/A by BET) (Å)	162.8	87.1

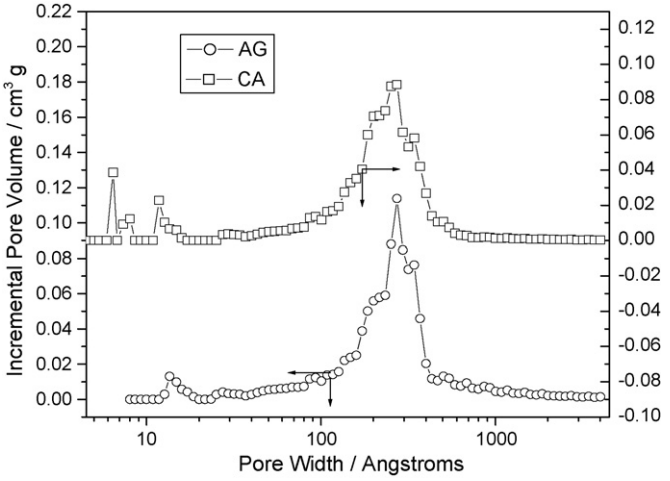

Fig. 2. Pore size distribution of the AG and CA.

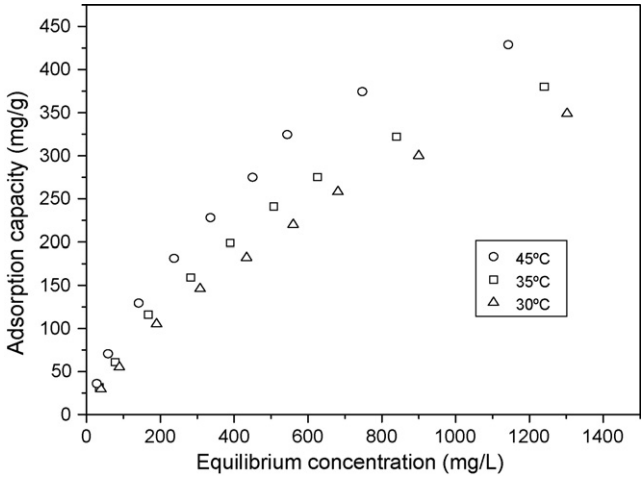

Fig. 3. Adsorption isotherms of CA.

3.2. Adsorption isotherm studies

Adsorption isotherms of RBRX were determined on the basis of batch analysis at 30, 35 and 45 °C using a series of concentration dye solutions at fixed adsorbent mass and volume with 24 h of contact time. It was found from Figs. 3 and 4 that the adsorption of RBRX increased with temperature from 30 to 45 °C. The increase in adsorption capacity of aerogels with temperature indicates an endothermic process. Several isotherm equations are available and two of them were selected in this study, Langmuir and Freundlich isotherms, at the same time, adsorption isotherm data of dye were fitted to well-known and widely applied isotherm models of Langmuir and Freundlich. The Langmuir isotherm is based on the assumption that adsorption takes place at specific homogeneous sites within the adsorbent and there is no significant interaction among adsorbed species and that the adsorbent is saturated after one layer of adsorbent

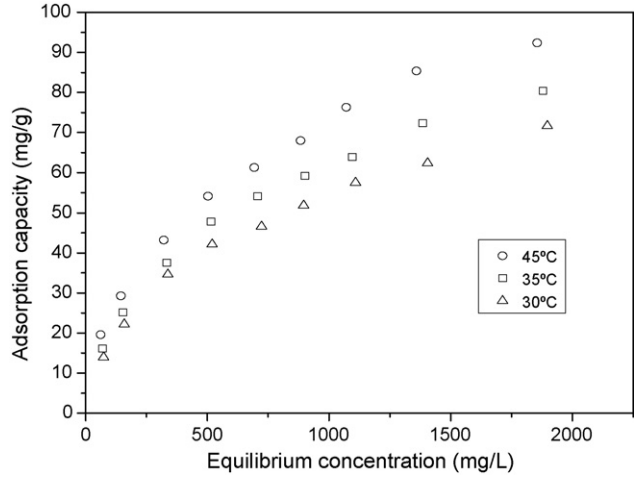

Fig. 4. Adsorption isotherms of AG.

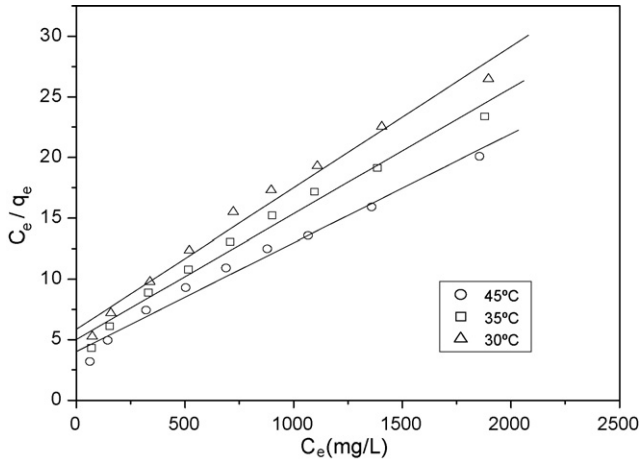

Fig. 5. Langmuir plots for adsorption of dye on AG.

molecules formed on the adsorbent surface. The linearized Langmuir isotherm equation can be written as follows [23]:

$$\frac{C_e}{q_e} = \frac{1}{q_0 b} + \frac{C_e}{q_0} \quad (2)$$

where q_e (mg/g) is the adsorption capacity, C_e (mg/L) is the equilibrium concentration of solute, q_0 (mg/g) is the maximum capacity of adsorbate to form a complete monolayer on the surface, b (L/mg) is the Langmuir constant related to the heat of adsorption. When C_e/q_e is plotted against C_e and the data are regressed linearly, q_0 and b constants can be calculated from the slope and the intercept. Langmuir plots are shown in Figs. 5 and 6, and according to the experimental data, the Langmuir plot is fit for the experimental data. Values of q_0 and b are presented in Table 2. The values of b increased with temperature, indicating that the adsorption of RBRX on AG and CA increased with temperature. The results implied that the affinity of the binding sites for RBRX increased with the temperature. It is obviously found that the maximum capacity q_0 of CA are much bigger than the q_0 of AG. The main reason is that the micropore surface area and volume of the CA is great larger than that of relevant AG. These micropores in the CAs are mainly produced

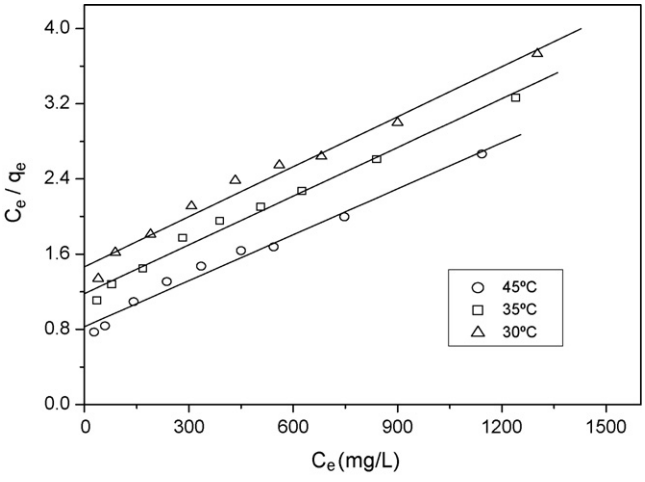

Fig. 6. Langmuir plots for adsorption of dye on CA.

Table 2
Isotherm parameters for removal of RBRX dye by AG and CA

Langmuir constants			
Temperature (°C)	R^2	q_0 (mg/g)	b (L/mg)
30 (CA)	0.99020	565	0.00131
35 (CA)	0.99349	578	0.00147
45 (CA)	0.99151	609	0.00199
30 (AG)	0.99049	86	0.00198
35 (AG)	0.99067	97	0.00205
45 (AG)	0.99068	112	0.00223
Freundlich constants			
Temperature (°C)	R^2	K_f ($mg^{1-(1/n)}$ $L^{1/n}$ g^{-1})	$1/n$ (Dimensionless)
30 (CA)	0.99721	2.185	0.72448
35 (CA)	0.99609	2.831	0.70628
45 (CA)	0.99513	4.29	0.67625
30 (AG)	0.99577	1.783	0.49541
35 (AG)	0.99751	2.135	0.48813
45 (AG)	0.99846	2.825	0.47208

during carbonization which we discussed previously. It is well known that the mesopores act chief function of mass transport and the micropores provide largely active adsorption sites, therefore, the increasing micropore during carbonization can largely enhance the adsorption capacity of the CA. The experimental adsorption capacity (q_e) is less than the maximum adsorption capacities (q_0), and this is probably due to some unoccupied active adsorption sites left under the experimental concentration.

The essential characteristics of the Langmuir isotherm can be expressed by a dimensionless constant called equilibrium parameter R_L, which splendidly determines the favorability and the shape of the isotherm of the adsorption process by applying the equation [4]:

$$R_L = \frac{1}{(1 + bC_0)} \quad (3)$$

where b is the Langmuir constant, C_0 is the initial dye concentration (mg/L), and R_L values indicate the type of isotherm. The value of R_L indicates the type of the isotherm to be either unfavorable ($R_L > 1$), linear ($R_L = 1$), favorable ($0 < R_L < 1$), or irreversible ($R_L = 0$). All values of R_L calculated in the above equation were found to be in the range of 0.183–0.884 (not presented in Table 2), indicating that the adsorption process is favorable for both adsorbents.

The Freundlich isotherm model takes the multilayer and heterogeneous adsorption into account. Its linearized form can be given as follows [24]:

$$\log q_e = \log K_f + \frac{1}{n} \log C_e \quad (4)$$

where q_e and C_e have the same definitions as in Langmuir equation above. Freundlich constant, K_f ($mg^{1-(1/n)}$ $L^{1/n}$ g^{-1}) is related to the adsorption capacity of aerogels and $1/n$ is another constant related to the surface heterogeneity. When $\log q_e$ was plotted against $\log C_e$ and the data were treated by linear regression analysis, Freundlich plots were shown in

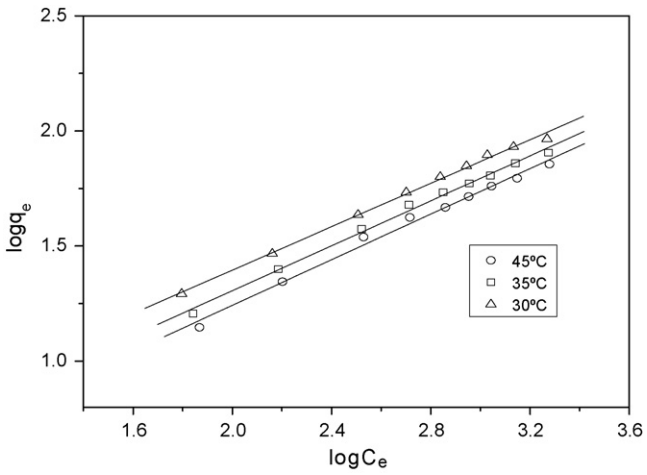

Fig. 7. Freundlich plots corresponding to adsorption of dye on AG.

Figs. 7 and 8, along with the experimental data. The correlation coefficients (R^2) of Freundlich were higher than 0.995. Thus, Freundlich plots are better satisfactorily with the experimental data. The $1/n$ and K constants were determined from the slope and intercept and listed in Table 2. The results illuminate that the K_f increased with temperature, indicating that the adsorption capacity increased with the temperature. Like K_f, n increased with temperature. If the n is below unity, then the adsorption is chemical. Otherwise, the adsorption is physical. All values of n exceeded unity, suggesting that the adsorption of RBRX is physical. The lower value of $1/n$ corresponded greater heterogeneity of the adsorbent surface. As shown in Table 2, the degree of heterogeneity of the AG and CA surface increased as the temperature increased. Values of $1/n$ are between 0 and 1, confirming that the adsorption processes are favorable.

In conclusion, all R^2 values exceeded 0.99 for both the Langmuir and the Freundlich models, suggesting that both models closely fitted the experimental results. However, applicability of these isotherm equations was compared by calculating a correlation coefficient. It can be seen that the Freundlich model (R^2 higher than 0.995) yielded a little better fit than the Langmuir model (R^2 higher than 0.990) for the adsorption of RBRX onto AG and CA. It is also evident from these data that the surface of AG and CA is made up of heterogeneous adsorption patches than homogenous adsorption patches. Both the Langmuir and the Freundlich models suggest that increasing temperature increased adsorption capacity, revealing that the adsorption is endothermic. The following section presents the detailed thermodynamic parameters.

3.3. Adsorption thermodynamic study

From the Langmuir parameter b at different temperatures, we can also estimate the thermodynamic parameters. Thermodynamic data such as adsorption energy can be obtained from Langmuir equations. The Langmuir constant b is related to the enthalpy of adsorption. Therefore, the thermodynamic parameters including the free energy change (ΔG°), enthalpy change (ΔH°) and entropy change (ΔS°) were also evaluated using the following equations:

$$-\Delta G^\circ_{ads} = RT\ln(b) \quad (5)$$

$$\ln b = \frac{\Delta S^\circ}{R} - \frac{\Delta H^\circ}{RT} \quad (6)$$

where ΔG° is the free energy change ($J\,mol^{-1}$), T is the absolute temperature (K), R is the universal gas constant ($8.314\,J\,K^{-1}/mol$), and b is the Langmuir constant. ΔH° and ΔS° were calculated from the slope and intercept of van't Hoff plots of $\ln b$ versus $1/T$ (see Fig. 9). The results of ΔG°, ΔH°, and ΔS° were listed in Table 3. The negative values of ΔG° indicated the feasibility and spontaneous nature of the adsorption of RBRX on the adsorbent. The standard enthalpy change (ΔH°) for the adsorption on AG and CA was positive, indicating that the process was endothermic in nature. The adsorption of dye on adsorbents involves several processes, diffusion, and surface reaction. The increase in adsorption with temperature may be attributed to two factors, one is that the increase in the number of active surface sites is available for adsorption on the adsorbent, and the other is the desolvation of the adsorbing species and the decrease in the thickness of the boundary layer

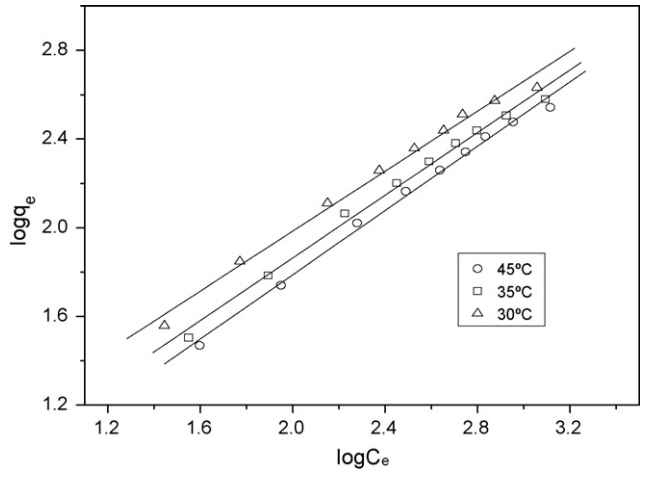

Fig. 8. Freundlich plots corresponding to adsorption of dye on CA.

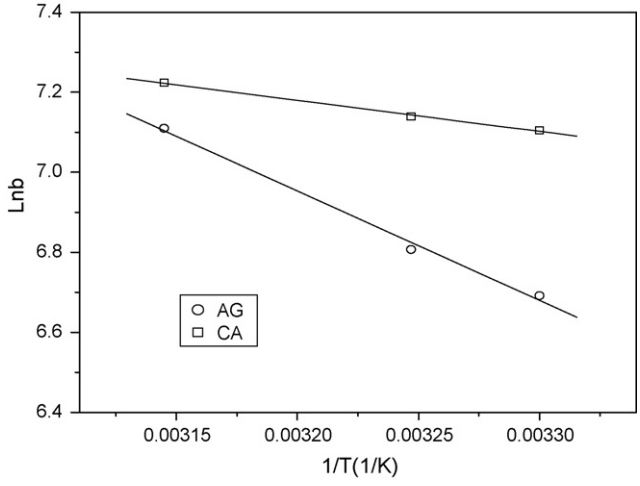

Fig. 9. Plot of lnb vs. 1/T for estimation of thermodynamic parameters.

Table 3
Equilibrium constants and thermodynamic parameters for the adsorption of RBRX on AG and CA

Sample	Temperature (K)	$b \times 10^{-3}$(L/mol)	ΔG(kJ/mol)	ΔS (kJ/mol K)	ΔH (kJ/mol)
CA	303	0.806	−16.857	0.131	22.735
	308	0.904	−17.430		
	318	1.224	−18.797		
AG	303	1.218	−17.897	0.0803	6.442
	308	1.261	−18.282		
	318	1.371	−19.098		

surrounding the adsorbent with increasing temperature, so that the mass transfer resistance of adsorbate in the boundary layer decreases. At higher temperature, the possibility of diffusion of solute within the pores of the adsorbent, and an affinity of the adsorbent toward RBRX would be increased. Since diffusion is an endothermic process, greater adsorption will be observed at higher temperature. Thus, the diffusion rate of dye in the external mass transport process increases with temperatures. The above results are further substantiated by the various thermodynamic parameters evaluated of adsorption. The positive value of ΔS° shows increased disorder at the solid–solution interface during the adsorption of dye under the experimental conditions. The adsorption increases randomness at the solid–solution interface with some structural changes in the adsorbate and adsorbent, and an affinity of the adsorbent toward RBRX. Therefore, the entropic change occurring from adsorption is negligible.

3.4. Adsorption kinetic considerations

Kinetics is another important aspect in any evaluation of sorption as a unit operation. The kinetic constants of dye adsorption could be used to optimize the residence condition. The influences of contact time on adsorption property of AG and CA are presented in Fig. 10. Fig. 10 presented that the velocity of attaining equilibrium on AG was quicker than that on CA, but the adsorption capacity of AG is lower greatly than that of CA. The time profile of dye uptake was a single, smooth and continuous curve leading to saturation, suggesting the adsorption process was slowly. For AG, the adsorption capacity is 50% on about 30 min and 90% on about 420 min of the equilibrium adsorption capacity. For CA, adsorption capacity is 50% on about 180 min and 90% on about 840 min of the equilibrium adsorption capacity. It is evident that the CA needs more time to reach adsorption equilibrium than AG. Generally speaking, three consecutive mass transport steps are associated with the adsorption of solute from solution by porous adsorbent. First, the adsorbate migrates through the solution to the exterior surface of the adsorbent particles by molecular diffusion, i.e., film diffusion, and then followed by solute movement from particle surface into interior site by pore diffusion, finally the adsorbate is adsorbed into the active sites at the interior of the adsorbent particle. This phenomenon takes relatively long contact time. The fact is that CA is composed of porous structure with large internal surface area. Thus, CA can accomplish three consecutive mass transport steps. But AG cannot accomplish completely the process because of lower internal surface area. Therefore, considering the structure of AG, the adsorption of dye on AG occurs only on the surface of AG, and can reach adsorption equilibrium faster than that of CA. The kinetic adsorption data is processed to understand the dynamics of adsorption process in terms of the order of rate constant. Kinetic data are treated with the pseudo-first-order kinetic model. The rate constant of adsorption is determined from the first order rate expression given by Lagergren and Svenska [25].

$$\log(q_e - q_t) = \log q_e - \frac{k_1}{2.303} t \quad (7)$$

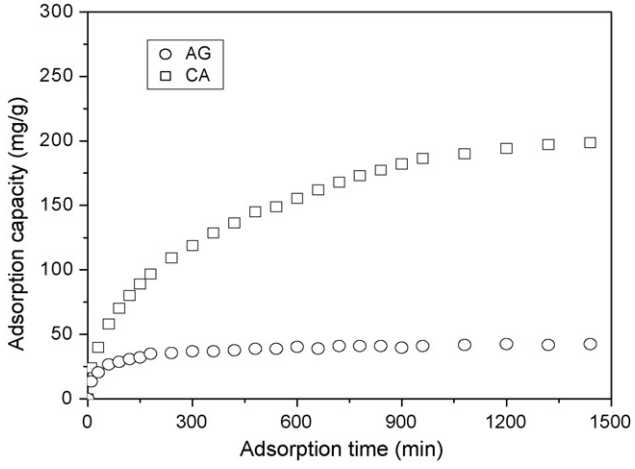

Fig. 10. Equilibrium curves for adsorption of RBRX onto AG and CA.

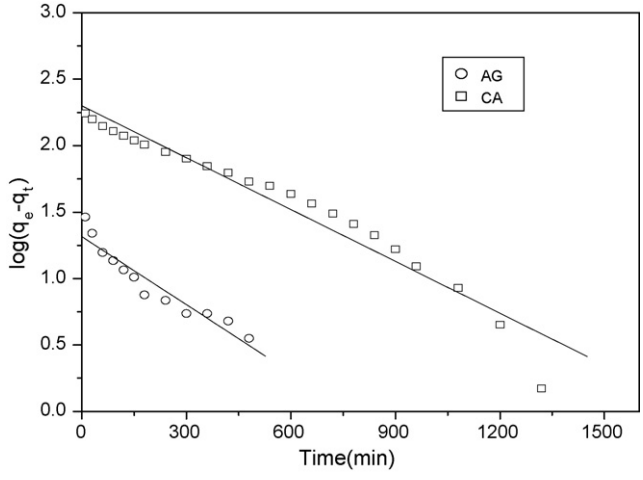

Fig. 11. Pseudo-first-order kinetics for adsorption of RBRX Dye on AG and CA.

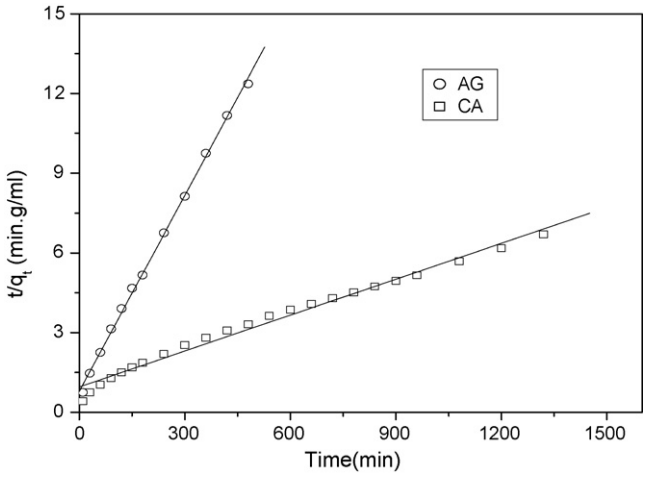

Fig. 12. Pseudo-second-order kinetics for adsorption of RBRX Dye on AG and CA.

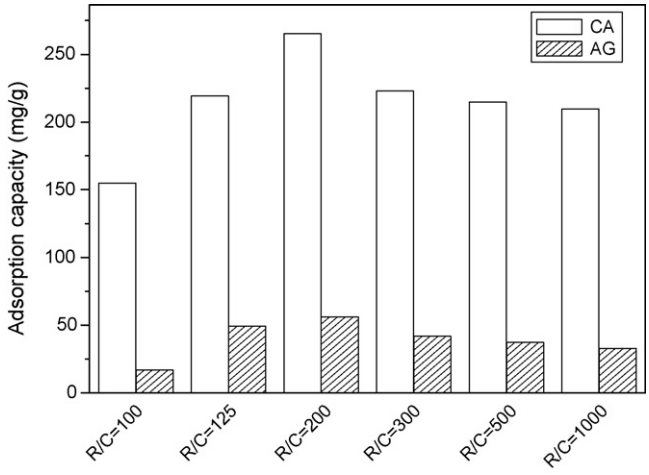

Fig. 13. The effect of the R/C on the adsorption property.

where q_e and q_t are the amounts of dye adsorbed (mg/g) at equilibrium and at time t (min), respectively, and k_1 is the rate constant of adsorption (L/min). Values of the rate constant, k_1, equilibrium adsorption capacity, q_e, and the correlation coefficient, R^2, are calculated from the plots of log $(q_e - q_t)$ versus t (Fig. 11) for CA sample. The correlation coefficients are found to be higher than 0.98, the calculated equilibrium adsorption capacities agree very well with experimental values (Table 4). This indicates that adsorption of RBRX Dye onto CA is an ideal pseudo-first-order reaction. However, although the correlation coefficients for AG are found to be higher than 0.96, the calculated equilibrium adsorption capacity do not agree with experimental values (Table 4). This indicates that adsorption of Reactive RBRX onto AG is not an ideal pseudo-first-order reaction.

Kinetic data were further treated with the pseudo-second order kinetic model [26]. If pseudo-second-order kinetics is applicable, the plot of t/q_t versus t should show a linear relationship. The second-order kinetic model is expressed as

$$\frac{t}{q_t} = \frac{1}{k_2 q_e^2} + \frac{1}{q_e} t \tag{8}$$

The equilibrium adsorption capacity (q_e), and the second-order constants k_2 (g/mg min) can be determined experimentally from the slope and intercept of plot t/q_t versus t (Fig. 12). The k_2 (g/mg min) and q_e (mg/g) values as calculated from Fig. 12 are listed in Table 4. Similar phenomena have been observed in the adsorption of AG and CA. From Fig. 12, we can see that the linear plots of t/q_t versus t show a good agreement with experimental data with the pseudo-second-order kinetic model for the two samples. The correlation coefficients for the second-order kinetic model are higher than 0.99. The calculated q_e values agree very well with the experimental data (Table 4). These results indicate that the adsorption of RBRX on AGs and CAs obeys pseudo-second-order kinetic model.

3.5. Study on influencing factors

3.5.1. Effect of R/C

The previous study showed that the pore structure and distribution of AGs and CAs could be controlled through adjusting R/C [21]. We can obtain the AG and CA samples with different BET specific surface areas, pore size distribution and pore shapes through the change of R/C during the process of the synthesize. The variations in adsorption capacity of the samples from RBRX solution at various R/C are shown in Fig. 13. Fig. 13 shows that the adsorption capacity increases firstly and then decreases with the R/C of AGs and CAs increases. It is evident that the maximum adsorption capacity of dye for the two types of samples is observed at R/C = 200. The reason could be that the AG and CA of R/C = 200 has maximum mesopore volume and mesopore surface areas among all samples [21].

3.5.2. Effect of initial pH

Solution pH affects the surface charge of the adsorbents as well as the degree of ionization of the materials present in the solution. Solution pH also affects the structural stability of RBRX, and therefore, its color intensity. Hence, the pH value of the dye solution plays an important role in the whole adsorption process and thus in influencing the adsorption capacity. Fig. 14 shows the effect of solution pH on RBRX dye adsorption

Table 4
Pseudo-first- and pseudo-second-order adsorption rate constants and the calculated and experimental q_e values for adsorption of RBRX on AG and CA

Sample	First-order kinetic model				Second-order kinetic model		
	q_e (exp) (mg/g)	k_1 (L/min) 10^{-3}	q_e (cal) (mg/g)	R^2	k_2 (g/mg min) 10^{-5}	q_e (cal) (mg/g)	R^2
CA	199	2.9939	200	0.98	2.1526	220	0.99
AG	42	3.9381	21	0.96	71.3271	42	0.99

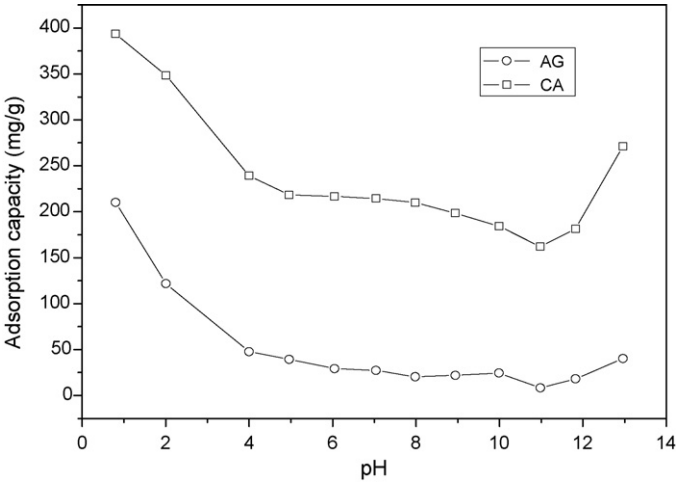

Fig. 14. The effect of the pH on the adsorption property.

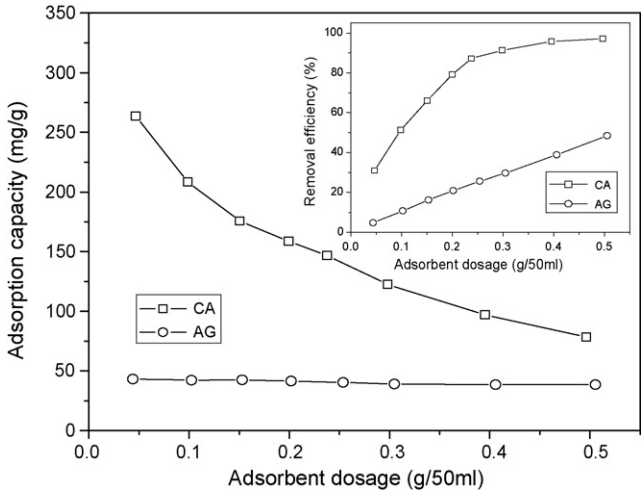

Fig. 15. The effect of adsorbent dose on the adsorption property.

efficiencies of AG and CA. When pH > 12 or pH < 4, the adsorptive capacity will be increased largely. Furthermore, the adsorption capacity of AG and CA in acid media is bigger than in basic media. Similar observations have been reported by other workers for adsorption of reactive dyes on coir pith activated carbon [3] indicating that the carbon materials has a net positive charge on its surface. As the pH of the adsorption solution was lowered, the positive charges on the surface increased. This would attract the negatively charged functional groups located on the reactive dyes [27]. Therefore, it has good results for adsorption of reactive dyes on AG and CA under lower pH conditions. In basic medium, besides improved adsorption arising from the possible reaction of dye with residual hydroxyl groups of CAs or AGs, the dye could also precipitate on the surface of nano-networks of the AGs and CAs, although no precipitate was found in the bottom of flask. As a result, the dye adsorption amount of CAs or AGs would increase and thus the concentration of dye would decrease in basic medium.

3.5.3. Effect of adsorbent dose

To optimize the adsorbent dose for the adsorption capacity and removal of RBRX from its aqueous solutions, adsorption was carried out with different adsorbent doses. The effect of adsorbent dose on the adsorption of RBRX on AG and CA are shown in Fig. 15. The dose of adsorbent was varied from 0.05 to 0.5 g/50 mL for AG and CA. It was observed that adsorption capacity of CA decreased greatly with increasing dose of adsorption. However, the adsorption capacity of AG decreased slightly with the adsorbent dose and reached a constant value after a particular dose. The inset of Fig. 15 presents the removal efficiency of RBRX from aqueous solution for AG and CA with different adsorbent doses. It showed more clearly that the removal efficiency of RBRX increased with increasing the amount of adsorbent for both the adsorbent. The effect of adsorbent dose on the adsorption process can be explained as follows: as the adsorbent dose increases, the removal efficiency of RBRX increases. Then the increase of removal efficiency results in the decreases of equilibrium concentration of RBRX. It is well known that the change of equilibrium concentration of RBRX is controlled by the adsorption capacity of adsorbent. Along with increasing the adsorbent dose, the degree of decrease in equilibrium concentration is great for CA because of its higher adsorptive capacity, but very little for AG because of its lower adsorptive capacity. Thus, when increasing adsorption dose, the adsorption capacity of CA decreased greatly but the adsorption capacity of AG decreased slightly and reached a constant value after a particular dose.

3.5.4. Effect of particle size

Experiments were conducted to evaluate the influence of adsorbent particle size for a constant weight on the adsorption of RBRX. In this experiment, six adsorbent particle sizes we chosen were 5–10, 10–20, 20–40, 40–100, 100–200 and >200 mesh, respectively. The results obtained were graphically represented in Fig. 16. It was clearly shown that the uptake of RBRX would increase with the decrease in adsorbent particle size, whether AG or CA was used as adsorbent. When the particle size decreased from 5–10 to 40–100 mesh, the adsorption amount increased from 56 to 329 mg/g for CA, and 27 to 59 mg/g for AG. An increase in capacity with decreasing particle size mainly

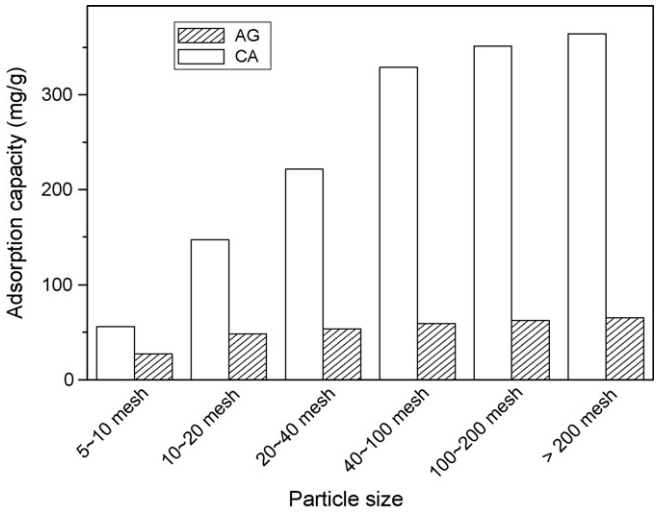

Fig. 16. The effect of the particle size on the adsorption property.

suggests that the dye molecules do not completely penetrate the particle or partly that the dye molecules preferentially adsorb near the outer surface of the particle. Considering the characteristics of porous materials that it would come into being a boundary layer to resists the adsorbate enter the interior of adsorbent in the process of adsorption. The adsorption is limited to the external surface area of the adsorbent. Therefore, the decreased particle size reduces the external mass transfer resistance and helps adsorbate to enter into the interior of adsorbent for contacting more active sites during the adsorption process.

4. Conclusions

In this study, AG and CA as adsorbents were successfully fabricated by a sol–gel polymerization method. The ability of AG and CA to adsorption RBRX was tested using equilibrium, kinetic and thermodynamic aspects. Adsorption experiments confirmed AG and CA are effective adsorbents for the adsorption of RBRX from aqueous solutions. Furthermore, CA had higher adsorption efficiency than AG. The Langmuir and Freundlich adsorption models were used to express the sorption phenomenon of the adsorbate. Equilibrium data agreed well with Langmuir and Freundlich model. Kinetic studies indicated that the adsorption of CA followed pseudo first and second order kinetic model, but the adsorption of AG followed pseudo first order kinetic model. The negative value of ΔG° confirmed the spontaneous nature adsorption process. The positive value of ΔS° showed the randomness at the solid–solution interface was increased during adsorption and the positive value of ΔH° indicated the adsorption process was endothermic. The adsorption of RBRX was found to be dependent on solution pH, R/C of adsorbent, adsorbent dose and adsorbent particle size.

Acknowledgements

This research was supported by the Project of NNSFC (50472029, 50632040), the Foundation of SRFDP, and the Scientific Foundation of Guangdong (2004A30404001).

References

[1] D. Peterson, J. Shore (Eds.), Colorants and Auxiliaries: Organic Chemistry and Application Properties, 1, BTTG-Shirley, Manchester, 1990, pp. 32–72.
[2] L.C. Morais, O.M. Freitas, E.P. Goncalves, L.T. Vasconcelos, G.C. Beca, Reactive dyes removal from wastewaters by adsorption on eucalyptus bark: variables that define the process, Water Res. 33 (1999) 979–998.
[3] K. Santhy, P. Selvapathy, Removal of reactive dyes from wastewater by adsorption on coir pith activated carbon, Bioresour. Technol. 97 (2006) 1329–1336.
[4] N. Sakkayawong, P. Thiravetyan, W. Nakbanpote, Adsorption mechanism of synthetic reactivedye wastewaterby chitosan, J. Colloid Interface Sci. 286 (2005) 36–42.
[5] M.S. Chiou, H.Y. Li, Adsorption behavior of reactive dye in aqueous solution on chemical cross-linked chitosan beads, Chemosphere 50 (2003) 1095–1105.
[6] J.A. Lazlo, Preparing an ion exchange resin from sugarcane bagasse to remove reactive dye from wastewater, Text Chem. Color 28 (1996) 13–17.
[7] K.S. Low, C.K. Lee, Quaternized rice husks as sorbent for reactive dyes, Bioresour. Technol. 61 (1997) 121–125.
[8] K.S. Low, C.K. Lee, K.L. Lee, Removal of reactive dyes by quaterniced coconut husk, J. Environ. Sci. Health. Part A: Environ. Sci. Eng. 33 (1998) 1479–1489.
[9] S. Karcher, A. Kommüller, M. Jekel, Anion exchange resins for removal of reactive dyes from textile wastewaters, Water Res. 36 (2002) 4717–4724.
[10] M.K. Purkait, S. DasGupta, S. De, Adsorption of eosin dye on activated carbon and its surfactant based desorption, J. Environ. Manage. 76 (2005) 135–142.
[11] J.J.M. Órfão, A.I.M. Silva, J.C.V. Pereira, S.A. Barata, I.M. Fonseca, P.C.C. Faria, M.F.R. Pereira, Adsorption of a reactivedye on chemically modified activated carbons—Influence of pH, J. Colloid Interface Sci. 296 (2006) 480–489.
[12] X. Yang, B. Al-Duri, Kinetic modeling of liquid-phase adsorption of reactive dyes on activated carbon, J. Colloid Interface Sci. 287 (2005) 25–34.
[13] W. Yang, R. Fu, Adsorption kinetics of theophylline on organic aerogels and carbon aerogels, Ion Exchange Adsorp. 2 (2006) 126–133.
[14] D. Wu, X. LIU., R. Fu, The adsorption of organic vapours on carbon aerogels and their precursor organic aerogels, New Carbon Mater. 4 (2005) 305–311.
[15] R.W. Pekala, Organic aerogels from the polycondensation of resorcinol with formaldehyde, J. Mater. Sci. 24 (1989) 3221–3227.
[16] M.S. Dresselhaus, Future directions in carbon science, Annu. Rev. Mater. Sci. 27 (1997) 1–34.
[17] J. Goel, K. Kadirvelu, C. Rajagopal, V.K. Garg, Investigation of adsorption of lead, mercury and nickel from aqueous solutions onto carbon aerogel, J. Chem. Technol. Biotechnol. 80 (2005) 469–476.
[18] J. Goel, K. Kadirvelu, C. Rajagopal, V.K. Garg, Removal of lead(II) from aqueous solution by adsorption on carbon aerogel using a response surface methodological approach, Ind. Eng. Chem. Res. 44 (2005) 1987–1994.
[19] A.K. Meena, G.K. Mishra, P.K. Rai, C. Rajagopal, P.N. Nagar, Removal of heavy metal ions from aqueous solutions using carbon aerogel as an adsorbent, J. Hazard. Mater. B122 (2005) 161–170.
[20] J. Goel, K. Kadirvelu, C. Rajagopal, V.K. Garg, Removal of mercury(II) from aqueous solution by adsorption on carbon aerogel: response surface methodological approach, Carbon 43 (2005) 195–213.
[21] D. Wu, R. Fu, M.S. Dresselhaus, G. Dresselhaus, Fabrication and nanostructure control of carbon aerogels via a microemulsion-templated sol–gel polymerization method, Carbon 44 (2006) 675–681.
[22] D. Wu, R. Fu, S. Zhang, M.S. Dresselhaus, G. Dresselhaus, Preparation of low-density carbon aerogels by ambient pressure drying, Carbon 42 (2004) 2033–2039.
[23] I. Langmuir, The adsorption of gases on plane surfaces of glass, mica and platinum, J. Am. Chem. Soc. 40 (1918) 1361–1403.
[24] H.M.F. Freundlich, Over the adsorption in solution, J. Phys. Chem. 57 (1906) 385–471.
[25] S. Lagergren, K. Svenska, About the theory of so-called adsorption of soluble substances, Handlinger 24 (1898) 1–39.
[26] G. McKay, Y.S. Ho, Pseudo-second order model for sorption process, Process. Process. Biochem. 34 (1999) 441–465.
[27] A. Bousher, X. Shen, R. Ansell, Removal of coloured organic matter by adsorption onto low-cost waste materials, Water Res. 31 (1997) 2084–2091.